

# Deriving Intrinsic Parameters of Photoinduced Electron Transfer Reaction from the Transient Effect Probed by Picosecond Time-Resolved Fluorescence Quenching

X. Allonas,<sup>1,4</sup> P. Jacques,<sup>1</sup> A. Accary,<sup>2</sup> M. Kessler,<sup>2</sup> and F. Heisel<sup>3</sup>

Received September 28, 1999; revised February 15, 2000; accepted February 16, 2000

Fluorescence quenching of a pyrylium salt (PDP<sup>2+</sup>) by toluene in acetonitrile gives rise to a nonexponential decay. This behavior is ascribed to the so-called transient effect occurring at high quencher concentrations for diffusion-controlled reactions. First, the Kalman filter was used to deconvolute the original signal from the experimental decay curve and the response function of the apparatus. This treatment led to a calculated deconvoluted decay curve which enabled the transient effect analysis to be conducted. This real decay curve was then analyzed using two models. The Smoluchowski–Collins–Kimball (SCK) model, applied to diffusion-controlled reactions, yielded the reaction radius  $r_{AD}$  and the intrinsic rate constant  $k_{act}$  of the bimolecular electron transfer reaction. The Marcus electron transfer/diffusion (ETD) model, which provides a powerful method to evaluate the electronic coupling  $H_{el}$  associate with the reaction, was also used but is more difficult to handle due to extensive computational needs. Finally, the adequacy of the two models (SCK and ETD) for analysis of the transient effect was addressed, as well as the appropriateness of the Kalman filter for fluorescence signal deconvolution.

**KEY WORDS:** Transient effect; deconvolution; pyrylium salt; electron transfer.

## INTRODUCTION

Electron transfer (ET) in solution has received considerable attention during the past decade. Experimental results concerning back electron transfer in fluid media have been nicely described by the Marcus theory [1,2] and have confirmed the theoretical prediction of the inverted

region (MIR), i.e., a decrease in the rate constant of reaction at high exergonicity [3–5]. However, in the case of forward electron transfer the situation remains unclear. The existence of the MIR has not been fully demonstrated and only a few papers report some vestiges [6,7]. In fact, generally, the experimental results agree fairly well with the Rehm–Weller empirical relationship [8], whereas the Marcus theory is not able to explain that the quenching rate constant of the excited state is diffusion-controlled even at high exergonicity. The challenge in this field is to understand the reason for the discrepancy between experiments and theory.

A possible way to interpret this discrepancy is to study the diffusion-controlled fluorescence quenching at high donor concentrations. Under such conditions nonexponential decays of fluorescence can be observed, a behavior called the transient effect [9–12]. This effect is

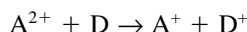
<sup>1</sup> Département de Photochimie Générale, UMR CNRS No. 7525, Ecole Nationale Supérieure de Chimie, 3 rue A. Werner, 68093 Mulhouse Cedex, France.

<sup>2</sup> Laboratoire Gestion des Risques Environnement, Université de haute Alsace, 25 rue de Chemnitz, 68200 Mulhouse, France.

<sup>3</sup> Groupe d'Optique Appliquée, Laboratoire PHASE, UPR No. 292, 23 rue du Loess, 67037 Strasbourg Cedex 2, France.

<sup>4</sup> To whom correspondence should be addressed. Fax: (33) 3 8933 6895. e-mail: X.Allonas@univ-mulhouse.fr

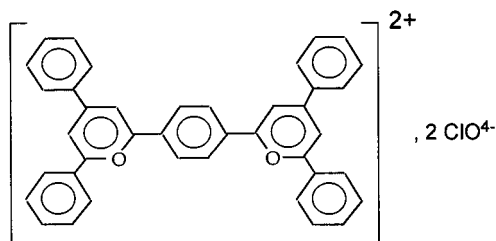
ascribed to the fast depletion of fluorescer molecules which react with neighboring quencher molecules at an earlier time after excitation. This occurs until a stationary distribution is reached and a pure diffusion-controlled reaction takes place. By fitting the decay curves with the help of appropriate models, one can retrieve some intrinsic parameters of the ET reaction. In recent years these methods have been used to evaluate the bimolecular rate constant of the reaction [13–17], the encounter distance between the reactants [15,17,18], the electronic coupling energy  $H_{el}$  [16,19], and the attenuation factor for electronic coupling,  $\beta$  [19,20]. Most of the studies deal with neutral reactants producing an attractive ion pair. No report is available on the behavior of charge shift systems or the generation of a repulsive ion pair through the following scheme:



In this paper the electron transfer reaction between a positively double-charged pyrylium salt  $PDP^{2+}$  and toluene was studied. At a high quencher concentration a transient effect was observed, resulting in a nonexponential decay. In the first stage, deconvolution of the decay curves was carried out using a Kalman filter. It was shown that this procedure leads to the recovery of the true decay curve, without assuming any analytical expression of it. Later, two models were applied to interpret this true decay, which enabled the evaluation of three important parameters of the ET process: the “activation rate constant” of reaction  $k_{act}$ , the distance of reaction  $r_{AD}$ , and the electronic coupling between reactants  $H_{el}$ . The classical Smoluchowski–Collins–Kimball (SCK) model yields  $r_{AD}$  and  $k_{act}$ , and the electron transfer/diffusion model (ETD) model leads to the value of the electronic coupling  $H_{el}$ .

## EXPERIMENTAL

The pyrylium salt  $PDP^{2+}$  (Scheme I), used as the starting material, was kindly donated by Dr. V. Wintgens (Laboratoire des Matériaux Moléculaires UPR 241, Thiais, France) [21]. Spectroscopic-grade acetonitrile from



Scheme 1.

Fluka was used as received, and toluene was distilled prior to its use. The lifetime of the singlet excited state of  $PDP^{2+}$  is 2.7 ns in acetonitrile, and the excitation energy is 2.64 eV. The reduction potential of  $PDP^{2+}$  measured by cyclic voltametry in acetonitrile, using 0.1 M tetraethylammonium hexafluorophosphate as a supporting electrolyte [22], was 0.15 V/SCE. The oxidation potential of toluene, measured under the same conditions, was estimated as 2.40 V/SCE.

For time-resolved fluorescence measurements, the excitation source was a mode-locked titane:sapphire laser (Spectra-Physics, Tsunami), pumped by an argon ion laser (Spectra-Physics 2030) and delivering pulses at 760 nm at a repetition rate of 82 MHz. After frequency doubling of the fundamental emission (using a nonlinear crystal), pulses of 150-fs duration and 0.75-nJ energy were obtained at 380 nm. The fluorescence, recorded at a right angle through an interference filter centered at 487 nm (maximum emission), was focused on the entrance slit of a streak camera consisting of a S20 photocathode image converter tube (ITL), which changes the temporal profile of the incoming light pulses into a spatial profile at the phosphor screen of the tube. The readout of the fluorescence decay was performed with a digitized video-camera (Photonetics GmbH; ARP KR10K) comprising a linear photodiode array of 512 pixels (Reticon) optically coupled to the streak camera phosphor.

The streak camera was operating in the synchroscan mode (all the electronic circuits were realized in the GOA) with adjustable time definitions. The time calibration was carried out by the usual Fabry–Perot standard method. A time width of 2.86 ps/pixel (channel) was used. The FWHM of the experimental temporal resolution curve of the whole setup was equal to six channels; the resolution was limited by the spatial definition of the image converter tube. The true shape of the response function was obtained by recording the laser pulses under the same conditions as those used for fluorescence measurements.

The absorbance of the sample solution at the excitation wavelength was ca. 0.1 over 1 cm. The samples were deoxygenated by bubbling Ar for 15 min.

## DECONVOLUTION BY KALMAN FILTERING

Deconvolution of fluorescence decay curves is a delicate subject. Although many techniques have been developed in the past [23–25], the iterative convolution method is the most commonly used for the analysis of decay curves, since this technique is one of the most reliable provided that the decay law is known [26–28]. Other techniques have been reviewed recently [29,30],

but is the convolution of a response with a known decay law essential?

The authors suggest a Kalman filter [31] that enables the deconvolution of experimental curves without requiring the knowledge of any decay law  $P(t)$ . This approach yields a deconvoluted signal which can be used for the decay analysis.

From a mathematical point of view the experimental decay curve  $f(t)$  results from the convolution of the expected decay curve  $P(t)$  with the instrumental response function  $g(t)$ :

$$f(t) = \int_0^t g(t') \times P(t - t') dt' \quad (1)$$

Knowledge of  $g(t)$  is required to derive  $P(t)$  from experimental curves  $f(t)$ ; in fact  $g(t)$  is the response function of the apparatus obtained by sending the laser pulse diffused by a glass plate directly into the streak camera.

As the observed function  $f$  and  $g$  are discretized during the process,  $g(t)$  is replaced by a vector  $g_k$ ,  $k = 0, \dots, N$ , and  $f(t)$  by a vector  $f_k$ ,  $k = 0, \dots, M$ , with the proviso that  $M > N$ .  $M$  corresponds to the time duration of the decay curve and  $N$ , the length of the pulse response, is a constant dependent on the optical and electronic performances of the apparatus. The sampling time  $\Delta t = t_{k+1} - t_k$  is the inverse of the measurement frequency.

The convolution integral (1) can be written

$$f_k = \sum_{j=\max(0, k-N)}^k g_{k-j} P_j \Delta t \quad (2)$$

that can be viewed as a matrix product:

$$F = GP \quad (3)$$

$$\begin{pmatrix} f_0 \\ f_1 \\ \dots \\ f_M \end{pmatrix} = \begin{bmatrix} g_0 & 0 & 0 & \dots & 0 \\ g_1 & g_0 & 0 & & 0 \\ g_0 & g_1 & g_0 & & 0 \\ \dots & \dots & \dots & \dots & \dots \\ g_N & g_{N-1} & \dots & g_0 & 0 & \dots & 0 \\ 0 & g_N & g_{N-1} & \dots & g_0 & \dots & 0 \\ \dots & \dots & \dots & \dots & \dots & \dots & \dots \\ 0 & \dots & \dots & g_N & \dots & g_1 & g_0 \end{bmatrix} \times \begin{pmatrix} P_0 \\ P_1 \\ \dots \\ P_M \end{pmatrix} \quad (3')$$

To determine  $P(t)$ , a term  $W$  expressing the experimental measurement error was included, so that

$$F = GP + W, \quad \text{with} \quad W = (W_0, \dots, W_M) \quad (4)$$

The vector components  $W_k$ ,  $k = 0, \dots, M$ , are uncorrelated, zero mean random variables.  $P$  was reconstructed using a classical linear Kalman filter [31]. The Kalman filter is well suited to solve Eq. (4) because inversion of matrix  $G$  is not possible due to the very low value of its determinant  $\det [G]$ . The Kalman filter provides the best solution  $\hat{P}$  of  $P$  in the sense that  $(F - G\hat{P})^T(F - G\hat{P})$  is small.

The estimate  $\hat{P}$  is the computed value of the quantity  $P$ , based upon a set of measurements  $F$ . This estimate must be unbiased, that is, its expected value  $IE(\hat{P}) = P$ . Moreover, it is possible to calculate the variance estimate i.e., the mean least-squares error:

$$\|\hat{P} - P\|_{L^2(P)} = IE[\sum_{k=0}^M (\hat{P}_k - P_k)^2] \quad (5)$$

The minimum variance estimate that gives this minimum is denoted  $\hat{P}_{vm}$ .

One can write

$$\hat{P}_{vm} = \arg_{\rho_{unbiased}} \inf \|\hat{P} - P\|_{L^2(P)} \quad (6)$$

The Kalman filter is constructed on the conditional estimator,

$$\hat{P}_{vm} = IE(P|F) \quad (7)$$

by calculating the successive quantities

$$IE(P|f_0), \quad IE(P|f_0, f_1), \dots, \quad IE(P|f_0, f_1, \dots, f_M) \quad (8)$$

In such a case, one can prove that  $\hat{P}_{vm}$  is a linear combination of the vector components  $f_0, f_1, \dots, f_M$  and is the projection in  $L^2(P)$  of  $P$  on the span  $(f_0, \dots, f_M)$ . Additional details can be derived from the optimal linear filtering [32], in particular, as regards the discrete Kalman filter that was implemented in the software.

Figure 1 shows an example of the deconvolution using the Kalman filter. It can be seen that the recovered fluorescence signal grows in fewer than six channels, i.e., 17 ps. This makes the deconvolution method reliable. Oscillations that appear in this signal can be ascribed to a slight difference between the recording wavelength of the response function (380 nm) and that of the fluorescence decay (487 nm) [26–30]. However, in spite of this minor defect, this procedure circumvents the classical problem of time shift, as time zero is accurately given by the fast ascending part of the signal.

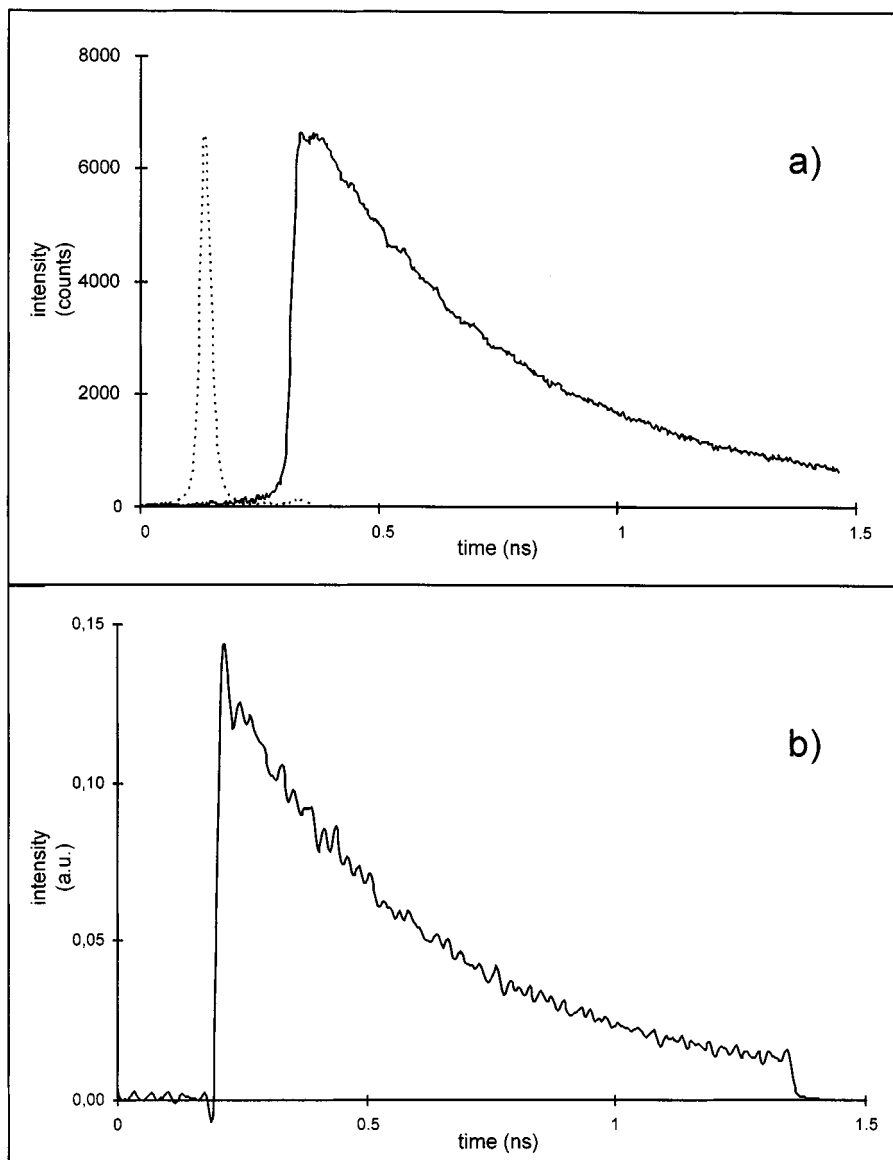


**Fig. 1.** (a) Experimental decay curves of the singlet state of  $\text{PDP}^{2+}$  quenched by toluene (0.10 M) in acetonitrile (solid line) and response function of the apparatus (dotted line). (b) Deconvoluted decay curves obtained through Kalman filtering.

### SMOLUCHOWSKI-COLLINS-KIMBALL ANALYSIS

It has been shown that the fluorescence decay of a molecule in the presence of a quencher can be described by the well-known Smoluchowski-Collins-Kimball model [10,11,33], where the reaction is controlled by

diffusion. The decay of the fluorescence intensity  $P(t)$  can be written

$$P(t) = P_{\max} \exp\left(-t/\tau_0 - [Q] \int_0^t k(t') dt'\right) \quad (9)$$

where  $P_{\max}$  is the initial intensity and  $\tau_0$  the lifetime

of the excited state without quencher  $Q$ .  $k(t)$ , the time-dependent "rate constant" for the reaction, is expressed as follows:

$$k(t) = \frac{k_d k_{\text{act}}}{k_d + k_{\text{act}}} \left( 1 + \frac{k_{\text{act}}}{k_d} \exp(x^2) \text{erfc}(x) \right),$$

with

$$\text{erfc}(x) = \frac{2}{\sqrt{\pi}} \int_0^x \exp(-s^2) ds, \quad (10)$$

$$x = \frac{\sqrt{Dt}}{r_{\text{AD}}} \left( 1 + \frac{k_{\text{act}}}{k_d} \right)$$

In this equation  $k_d = 4\pi r_{\text{AD}} N' D$  is the diffusion rate constant,  $k_{\text{act}}$  the bimolecular activation rate constant of the reaction,  $D$  stands for the diffusion coefficient of the reactants,  $r_{\text{AD}}$  is the encounter distance, and  $N'$  the Avogadro number.

When  $x \gg 1$ , Eq. (10) reduces to

$$k(t) = \frac{k_d k_{\text{act}}}{k_d + k_{\text{act}}} \left( 1 + \frac{k_{\text{act}}}{k_d + k_{\text{act}}} \frac{r_{\text{AD}}}{\sqrt{\pi Dt}} \right) \quad (11)$$

The expression of the time-dependent fluorescence intensity becomes

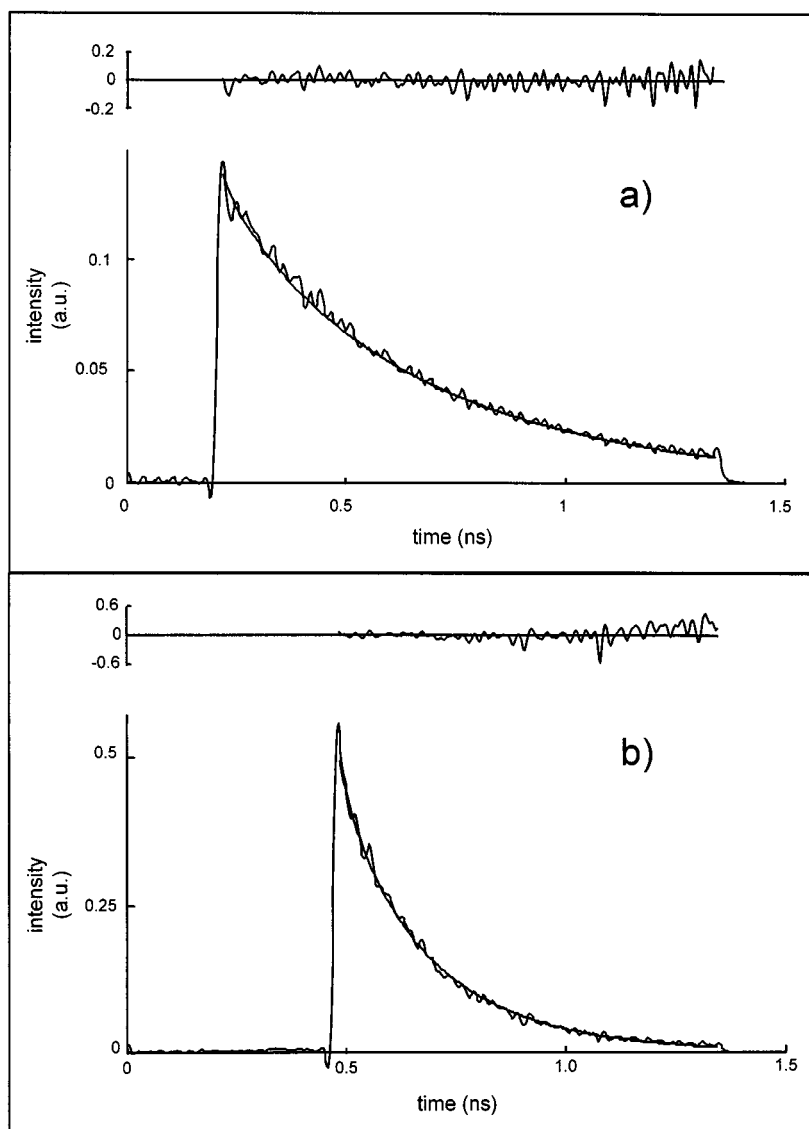


Fig. 2. SCK model fitting to deconvoluted  $\text{PDP}^{2+}$  fluorescence decay at (a) 0.10 M and (b) 0.30 M toluene.

$$P(t) = P_{\max} \exp(-(at + b\sqrt{t}), \quad \text{with}$$

$$a = \frac{1}{\tau_0} + \frac{k_{\text{act}}}{k_d + k_{\text{act}}} 4\pi r_{\text{AD}} D N' [Q] \quad \text{and} \quad (12)$$

$$b = 8 \left( \frac{k_{\text{act}} r_{\text{AD}}}{k_d + k_{\text{act}}} \right)^2 \sqrt{\pi D N' [Q]}$$

This expression represents the time-resolved fluorescence decay of the excited state.  $k_{\text{act}}$ ,  $r_{\text{AD}}$ , and  $D$  can be derived by correlating the experimental decays with this expression. It has been found, however, that the results are more reliable when the number of fitting parameters is reduced [13,17]. Therefore,  $D$  is generally estimated from the Stokes–Einstein relationship:

$$D = \frac{kT}{6\pi\eta r} \quad (13)$$

where  $\eta$  is the solvent viscosity and  $r$  the radius of the considered molecule. While the hard-sphere radius of toluene,  $r_D = 3.48 \text{ \AA}$ , was estimated from its molecular volume, that of  $\text{PDP}^{2+}$ ,  $r_A = 7.16 \text{ \AA}$ , was computed [34]. A Marquardt [35] minimization algorithm based on the mean least-squares method (LMS) was used to find the best fit for each experimental decay.

According to the estimations, the SCK model fits the experimental decays fairly well, as shown in Fig. 2. The values of  $k_{\text{act}}$  and  $r_{\text{AD}}$  are shown in Table I. Changing the donor concentration does not significantly affect the values, which remain stable within experimental error. The free energy change for the ET reaction  $\Delta G_{\text{et}}$  can be calculated according to

$$\Delta G_{\text{et}} = E_{\text{ox}} - E_{\text{red}} - E^* \quad (14)$$

by leaving out the repulsive coulombic term.  $E_{\text{ox}}$  is the oxidation potential of the donor,  $E_{\text{red}}$  the reduction potential of the acceptor, and  $E^*$  the energy of the excited state. In the present case, where  $\Delta G_{\text{et}} = -0.39 \text{ eV}$ , the reaction is slightly exergonic but remains in the normal region, and therefore, the reaction should occur when the reactants are in close contact. Indeed an average value for  $r_{\text{AD}}$  was found to be ca  $5.9 \pm 0.5 \text{ \AA}$  (Table I), a value lower than the sum of the radii of the reactants. This seems to imply that the encounter complex has a face-to-face geometry, thus increasing the electronic coupling between the involved orbitals (vide infra). Moreover, in this range of moderate exergonicity, the intrinsic rate constant should not be substantially higher than the diffusion limit. The experimental value of  $k_{\text{act}} = 1.2 \cdot 10^{11} \text{ M}^{-1} \text{ s}^{-1}$  is a reasonable one corresponding to that obtained for different systems [13–17]. In the SCK model it is assumed that the contribution to the bimolecular rate constant takes

place at an encounter distance close to  $r_{\text{AD}}$ , an hypothesis which was recently confirmed [36]. Under such conditions  $k_{\text{act}}$  can be related to the rate constant of the ET reaction  $k_{\text{et}}$  through the simplified relationship [37],

$$k_{\text{act}} = K k_{\text{et}}(r_{\text{AD}}) \quad (15)$$

where  $K$  is the equilibrium constant for the formation of the encounter complex at distance  $r_{\text{AD}}$ . In the present case, this constant can be calculated from the Fuoss–Eigen relationship:

$$K = \frac{4\pi N r_{\text{AD}}}{3000} \quad (16)$$

From the distance derived through the least-squares fitting ( $r_{\text{AD}} = 5.9 \pm 0.5 \text{ \AA}$ ), the value of the constant  $K$  is  $0.51 \text{ M}^{-1}$ . Finally, this leads to a first-order rate constant of the ET reaction equal to  $k_{\text{et}} = 2.3 \cdot 10^{11} \text{ s}^{-1}$ .

## ELECTRON TRANSFER/DIFFUSION (ETD) MODEL

A second analysis was performed on the same decay curves. In this recent approach, the decay of the fluorescence intensity can be expressed as follows [11,20, 36,38–40]:

$$P(t) = P_{\max} \exp\left(-\frac{t}{\tau_0} - 4\pi[Q]_{t=0} \int_d^\infty (1 - U(r, t)) r^2 dr\right) \quad (17)$$

$U(r, t)$  expresses the survival probability of the  $A^* - D$  pair as a function of the distance  $r$  between the reactants and time  $t$ . It was shown that if A and D undergo mutual diffusion,  $U(r, t)$  is diffusion-controlled [38,41] as in the ordinary diffusion of species in a cylindrical coordinate system:

$$\frac{\partial U(r, t)}{\partial t} = D \left( \frac{\partial^2}{\partial r^2} + \frac{2}{r} \frac{\partial}{\partial r} \right) U(r, t) - k_{\text{et}}(r) U(r, t) \quad (18)$$

The initial and boundary conditions were determined to

**Table I.** Parameter Values Obtained for Quenching of  $\text{PDP}^{2+}$  by Toluene

Toluene ( $M$ )	SCK			ETD	
	$\log k_{\text{act}}$	$r_{\text{AD}} (\text{\AA})$	$\chi^2$	$H_{\text{el}} (\text{meV})$	$\chi^2$
0.10	11.10	6.5	$3.6 \cdot 10^{-2}$	7.1	$3.4 \cdot 10^{-2}$
0.30	11.06	5.3	$1.6 \cdot 10^{-1}$	6.1	$2.3 \cdot 10^{-1}$

explain that the survival probability is highest at  $t = 0$  and when the distance  $r$  is great. It is also assumed that the growth rate probability is zero when the two species are in contact:

$$\begin{cases} U(r, 0) = 1 \\ U(\infty, t) = 1 \\ \left(\frac{\partial U}{\partial r}\right)_{r=r_0} = 0 \end{cases} \quad (19)$$

where  $r_0$  is the sum of the radii of the reactants. In Eq. (18) the rate constant of reaction  $k_{et}(r)$  is given by the semiclassical Marcus electron transfer equation:

$$k_{et}(r) = \frac{2\pi}{\hbar} H_{el}^2 \exp(-\beta(r - r_0)) \frac{1}{\sqrt{4\pi\lambda k_B T}} \exp\left[-\frac{(\lambda + \Delta G_{et})^2}{4\lambda k_B T}\right] \quad (20)$$

$\lambda$  is the reorganization energy calculated from

$$\lambda = \frac{\Delta e^2}{4\pi\epsilon_0} \left(\frac{1}{2r_A} + \frac{1}{2r_D} - \frac{1}{r}\right) \left(\frac{1}{n^2} - \frac{1}{\epsilon_s}\right) \quad (21)$$

$\epsilon_s$  and  $n$  are the permittivity and the refractive index of the solvent, respectively.

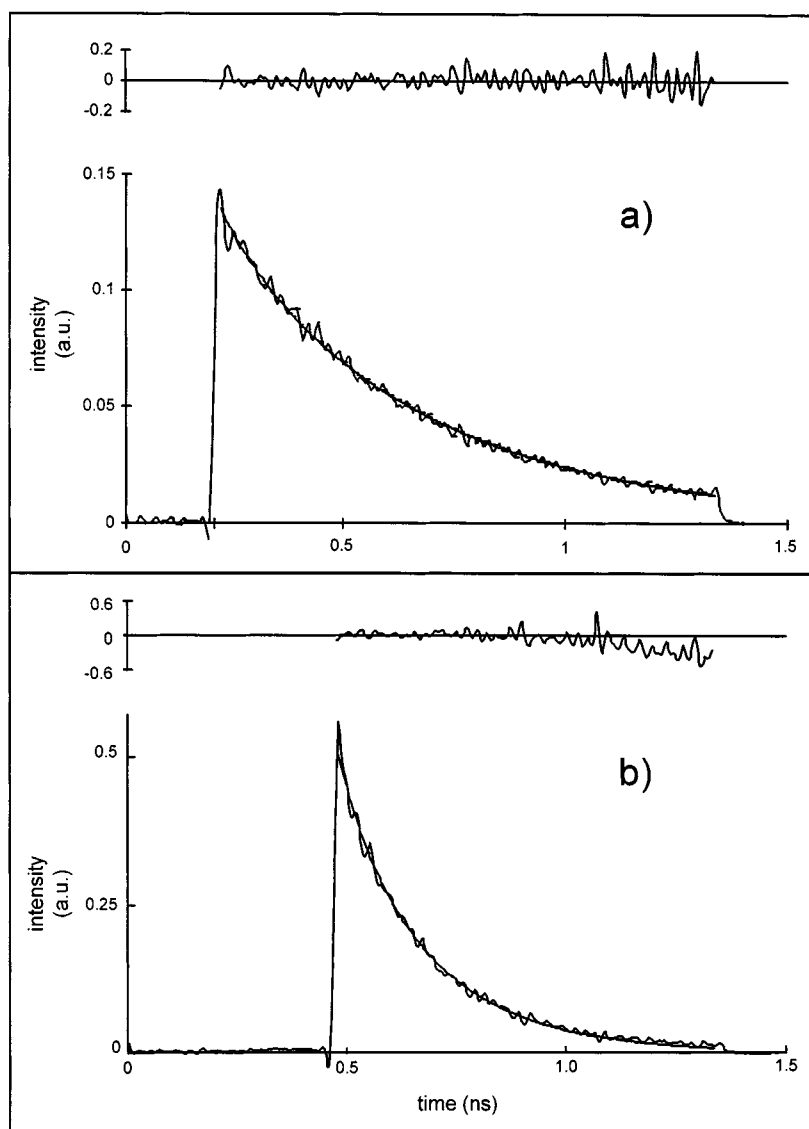


Fig. 3. ETD model fitting to deconvoluted PDP<sup>2+</sup> fluorescence decay at (a) 0.10 M and (b) 0.30 M toluene.

Equation (18) was solved by using the line method found in the ISML library [42]. The temporal region was divided into 500 equally spaced steps, and the spatial region was divided into 300 or 1000 steps without change in the calculated decays. After that, Eq. (17) was integrated using the trapezoidal approximation. A Marquardt algorithm was used to find the best estimates of the parameters. A first attempt was made to determine the value of two parameters, i.e.,  $H_{\text{el}}$  and  $\beta$ . Unfortunately, many local minima were observed from the least-squares fitting, depending on the values of the initial guesses and of the least-squares estimation criterion. This problem was recently addressed [19]. Therefore, it was deemed convenient to reduce the number of parameters by taking  $\beta$  equal to  $1 \text{ \AA}^{-1}$ , a value usually admitted in the literature [19,20,39,43].

Figure 3 shows that the ETD model closely fits the deconvoluted decay curves. The estimate residuals, reported in the upperpart of each panel, show a good agreement when the quencher is  $0.1 M$  and reveal that these values remain low when the quencher is  $0.30 M$ . The slight deviation observed at the end of the reaction could be accounted for by introducing a more sophisticated model [20,40] taking into account a two-particle radial distribution function, which is particularly important for high quencher concentrations. The  $\chi^2$  values obtained using the present method are close to those computed according to the SCK model (Table I). The values of  $H_{\text{el}}$  are 7.1 and 6.1 meV at 0.10 and 0.30  $M$  toluene, respectively. Besides being coherent, these two values demonstrate that the reaction is strongly nonadiabatic.

From  $H_{\text{el}}$  it is possible to estimate  $k_{\text{et}}(r)$  with Eq. (20) and the result is plotted in Fig. 4. It is apparent that the maximum rate constant is ca.  $3 \cdot 10^{11} \text{ s}^{-1}$  at reactant contact, i.e.,  $r_0 = r_{\text{A}} + r_{\text{D}} = 10.64 \text{ \AA}$ . This  $k_{\text{et}}(r_0)$  value is in good agreement with the  $k_{\text{et}}(r_{\text{AD}})$  as obtained from the SCK model. On the other hand, it should be kept in mind that if the ETD model is used, the reaction radius meets the condition  $r_{\text{AD}} \geq r_{\text{A}} + r_{\text{D}}$ , whereas the value of  $r_{\text{AD}}$  computed according to the SCK model does not support any assumption on the value of  $r_{\text{A}}$  or  $r_{\text{D}}$  except when calculating  $D$ . Therefore, the agreement as regards  $r_{\text{AD}}$  is only qualitative (reaction occurs at contact).

From a general point of view such comparative studies are both too sparse and nonexhaustive, so that one cannot decide which method is more appropriate when describing the transient effect.

## CONCLUSION

Quenching of the singlet excited state of  $\text{PDP}^{2+}$  by toluene at high concentrations leads to the observation of a transient effect on the fluorescence decay curves. A discrete Kalman filter was used to obtain deconvoluted decays from the experimental curves and the response function of the apparatus. From these decays, the transient effect was analyzed by two theoretical models. The classical Smoluchowski–Collins–Kimball model leads to the recovery of the reaction radius  $r_{\text{AD}}$  and the intrinsic rate constant of the reaction  $k_{\text{act}}$ . It was found that the reaction occurs at nearly  $5.9 \text{ \AA}$ , a shorter distance than the sum

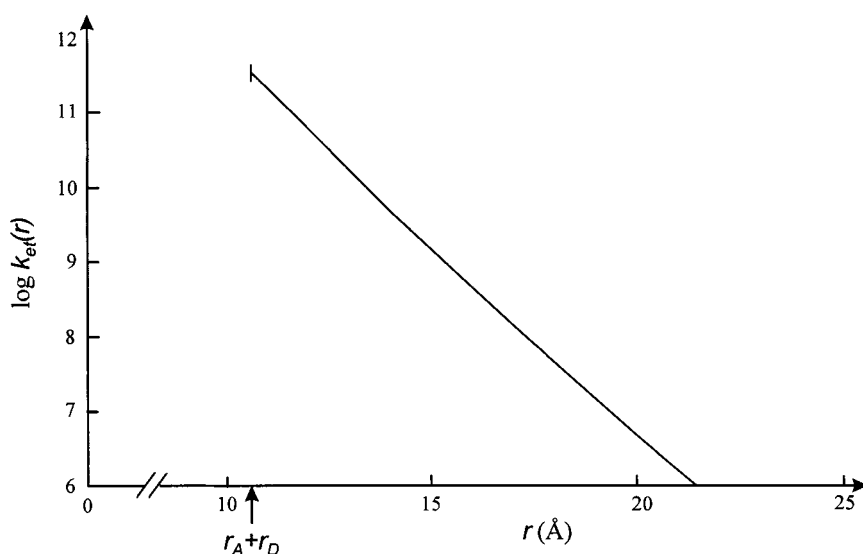


Fig. 4. Plot of  $k_{\text{et}}(r)$  according to Eq. (20),  $H_{\text{el}} = 6.6 \text{ meV}$ .



of the two radii of the reactants, which seems to imply that an efficient ET requires a face-to-face geometry. The rate constant of the reaction  $k_{\text{act}}$  is ca.  $1.2 \cdot 10^{11} \text{ M}^{-1} \text{ s}^{-1}$ , i.e., 10 times higher than the diffusion limit. The second model, based on the electron transfer theory, enables the calculation of the electronic coupling  $H_{\text{el}}$ . The value found in this case, i.e., 6.6 meV, shows that the reaction is strongly nonadiabatic. By calculating the distance dependence of the rate constant  $k_{\text{et}}$  for the electron transfer process, it was found that the reaction should occur at contact, a result in qualitative agreement with the conclusion derived from the SCK analysis. In addition, the relatively high value of  $H_{\text{el}}$  is in line with the necessity of a face-to-face arrangement found by using the SCK procedure. The transient effect can provide valuable information on the electron transfer step. However, the kinetics of fluorescence quenching partly controlled by diffusion is still an open question, and the corresponding theory undergoes constant modification. Thus, the authors believe that it makes no sense to determine which approach is more appropriate for treating the transient effect. After completing the present work they are inclined to consider that the SCK and ETD are complementary rather than competing methods.

## ACKNOWLEDGMENTS

Warm thanks are extended to Dr. V. Wintgens for suggesting PDP<sup>2+</sup> as a most efficient electron acceptor. A. Martz's technical help in fluorescence decay measurements is gratefully acknowledged.

## REFERENCES

1. R. A. Marcus (1956) *J. Chem. Phys.* **24**, 966.
2. R. A. Marcus and N. Sutin (1985) *Biochim. Biophys. Acta* **811**, 265.
3. I. R. Gould, D. Ege, and S. L. Mattes (1987) *J. Am. Chem. Soc.* **109**, 3794.
4. N. Mataga, T. Asahi, Y. Kanda, T. Okada, and T. Kakitani (1988) *Chem. Phys.* **127**, 249.
5. E. Vauthey, P. Suppan, and E. Haselbach (1988) *Helv. Chim. Acta* **71**, 93.
6. J. M. Chen, T. I. Ho, and C. Y. Mou (1990) *J. Phys. Chem.* **94**, 2889.
7. D. M. Guldi and K. D. Asmus (1997) *J. Am. Chem. Soc.* **119**, 5744.
8. D. Rehm and A. Weller (1970) *Isr. J. Chem.* **8**, 259.
9. A. Weller (1961) *Prog. React. Kinet.* **1**, 188.
10. R. M. Noyes (1961) *Prog. React. Kinet.* **1**, 129.
11. S. A. Rice (1985) *Comprehensive Chemical Kinetics, Vol 25. Diffusion Limited. Reactions*, Elsevier, New York.
12. J. C. Andre, M. Niclaude, and W. R. Ware (1978) *Chem. Phys.* **28**, 371.
13. S. Nishikawa, T. Asahi, T. Okada, N. Mataga, and T. Kakitani (1991) *Chem. Phys. Lett.* **185**, 237.
14. T. Kakitani, A. Yoshimori, and N. Mataga (1992) *J. Phys. Chem.* **96**, 5385.
15. P. Jacques and X. Allonas (1995) *Chem. Phys. Lett.* **233**, 533.
16. X. Allonas and P. Jacques (1997) *Chem. Phys.* **215**, 371.
17. S. Murata, M. Nishimura, S. Y. Matsuzaki, and M. Tachiya (1994) *Chem. Phys. Lett.* **219**, 200.
18. T. Niwa, K. Kikuchi, N. Matsusita, M. Hayashi, T. Katagiri, Y. Takahashi, and T. Miyashi (1993) *J. Phys. Chem.* **97**, 11960.
19. S. Murata, S. Y. Matsuzaki, and M. Tachiya (1995) *J. Phys. Chem.* **99**, 5354.
20. S. F. Swallen, K. Weidemaier, H. L. Tavernier, and M. D. Fayer (1996) *J. Phys. Chem.* **100**, 8106.
21. S. Tripathi, V. Wintgens, P. Valat, V. Toscano, and J. Kossanyi (1987) *J. Luminesc.* **37**, 149.
22. P. Jacques, D. Burget, and X. Allonas (1996) *New J. Chem.* **20**, 233.
23. D. V. O'Connor, W. R. Ware, and J. C. Andre (1979) *J. Phys. Chem.* **83**, 1333.
24. J. C. Andre, L. M. Vincent, D. V. O'Connor, and W. R. Ware (1979) *J. Phys. Chem.* **83**, 2285.
25. A. E. McKinnon, A. G. Szabo, and D. R. Miller (1977) *J. Phys. Chem.* **81**, 1564.
26. J. R. Lakowicz (1983) *Principles of Fluorescence Spectroscopy*, Plenum Press, New York.
27. M. Sikorski, E. Krystkowiak, and R. P. Steer (1998) *J. Photochem. Photobiol. A Chem.* **117**, 1.
28. M. Sikorski, W. Augustiniak, I. V. Khmelinskii, and F. Wilkinson (1996) *J. Luminesc.* **69**, 217.
29. M. Van Zegel, N. Boens, D. Daems, and F. C. De Schryver (1986) *Chem. Phys.* **101**, 311.
30. R. Das and N. Periasamy (1989) *Chem. Phys.* **136**, 361.
31. A. Gelb, J. F. Kasper, R. A. Nasdh, C. F. Price, and A. A. Sutherland (1974) *Applied Optimal Estimation*, MIT Press, Cambridge, MA, and Condon, England.
32. N. V. Ahmed (1988) *Element of Finite Dimensional Systems and Control Theory*, Longman Scientific and Technical, copublished with John Wiley & Sons, New York, Longman Group UK Ltd., Longman House, Burut Hill, Harlow.
33. F. C. Collins and G. E. Kimball (1949) *J. Colloid Sci.* **4**, 425.
34. The ground-state geometry of PDP<sup>2+</sup> was optimized by using the MNDO Hamiltonian from the Hyperchem package (Hypercube Inc., Canada). The radius was then derived from the calculation of the volume using a grid method.
35. D. W. Marquardt (1993) *J. Soc. Indust. Appl. Math.* **11**, 431.
36. L. Burel, M. Mostafavi, S. Murata, and M. Tachiya (1999) *J. Phys. Chem.* **103**, 5882.
37. G. M. Brown and N. Sutin (1979) *J. Am. Chem. Soc.* **101**, 883.
38. M. Tachiya (1983) *Radiat. Phys. Chem.* **21**, 167.
39. L. Song, S. F. Swallen, R. C. Dorfman, K. Weidemaier, and M. D. Fayer (1996) *J. Phys. Chem.* **97**, 1374.
40. S. F. Swallen, K. Weidemaier, and M. D. Fayer (1996) *J. Chem. Phys.* **104**, 2976.
41. H. Sano and M. Tachiya (1979) *J. Chem. Phys.* **71**, 1276.
42. From ISML library, trademark of Visual Numerics Inc., Houston, TX.
43. G. J. Kavarnos and N. J. Turro (1986) *Chem. Rev.* **86**, 401.